Journal of the Ceramic Society of Japan 115 [12] 925–928 (2007)

Paper

Sol–gel Synthesis of Macroporous YAG from Ionic Precursors via Phase Separation Route

Yasuaki TOKUDOME, Koji FUJITA,*,** Kazuki NAKANISHI, Kazuyoshi KANAMORI, Kiyotaka MIURA,* Kazuyuki HIRAO* and Teiichi HANADA

Department of Chemistry, Graduate School of Science, Kyoto University, Kitashirakawa, Sakyo-ku, Kyoto 606–8502
**Department of Material Chemistry, Graduate School of Engineering, Kyoto University, Katsura, Nishikyo-ku, Kyoto 615–8510*
***PRESTO, Japan Science and Technology Agency (JST), 4–1–8, Honcho Kawaguchi, Saitama 332–0012*

Yttrium aluminum garnet, $Y_3Al_5O_{12}$, (YAG) monoliths with well-defined macropores have been prepared from ionic precursors using the sol–gel method accompanied by phase separation. The addition of propylene oxide to the starting solution controls the gelation, while the addition of poly(ethylene oxide) induces the phase separation. Polymerization-induced phase separation and gelation concur by an appropriate selection of the starting composition, which allows the production of bicontinuous macroporous nanocomposite gels in large dimensions ($\sim 10 \times 10 \times 10$ mm^3). During heat treatment at 800°C, the monolithic nanocomposite gels crystallize into YAG without the formation of any intermediate phases or the precipitation of impurity phases, indicating higher homogeneity of cation distribution in the dried gels. The macroporous YAG network was maintained even after heat treatment at 1000°C for 10 h. [Received September 23, 2007; Accepted November 15, 2007]

Key-words : *Sol–gel method, Phase separation, Propylene oxide, Mixed metal oxide, Porous material*

1. Introduction

The sol–gel-derived porous materials have been utilized in an extended application such as catalyst, sensors, separation media, optical and electronic devices and so forth, because the versatility of sol–gel processing provides a means of controlling the shape, morphology and textual properties of the final material. Among some synthetic strategies, the sol–gel process accompanied by phase separation has been adopted to fabricate a variety of oxide systems with controlled porous structures. It has been well established for alkoxy-derived pure silica and silica-based sol–gel systems in which polymerization-induced phase separation and concurrent sol–gel transition produce monolithic materials with well-defined macroporous structures.[1),2)] Recently, pure titania and zirconia monoliths with well-defined macropores have been also synthesized via the phase separation route using the metal alkoxides as precursors.[3),4)]

On the other hand, recent advance of the metal-salt-derived gel-forming process assisted by the ring-opening reaction of an organic epoxide offers us new opportunities for the structural control of non-silica and silicate systems because of no need for highly reactive metal alkoxides.[5)] In the alkoxide-free sol-gel process, epoxides are utilized as the acid scavenger to raise the solution pH gradually, which drives the hydrolysis and condensation of hydrated metal species. Very recently, we have successfully prepared macroporous pure alumina monoliths by combining the phase separation route with the metal-salt-derived sol–gel process.[6)]

Extending the synthetic procedure of macroporous pure alumina, this paper demonstrates a trial of producing macroporous structures in non-silicate, mixed metal oxide systems. Since the metal-salt-derived sol–gel process has also proven useful in designing the precursor gels of highly homogeneous binary oxides,[7)] if combined with the phase-separation route, the formation of well-defined macropores would be possible even in mixed oxide systems. In this study, an Y-Al mixed metal oxide system is chosen as a representative because the difference of the reactivity between Y^{3+} and Al^{3+} in aqueous and/or ethanolic solution is relatively small. We show that Y–Al–O precursor gel monoliths with well-defined macropores can be prepared by the metal-salt-derived sol–gel process accompanied by phase separation and that the gel skeletons are converted into nanocrystalline YAG by heat treatment at temperature above 800°C without spoiling the macroporous morphology. Various synthetic approaches including templating techniques have been used to fabricate porous mixed metal oxides, but most of the porous materials were dried to powders.[8)–13)] Using the present technique, large-dimension, mixed metal oxide monoliths with controlled porous structures can be prepared via a spontaneous chemical process without the aid of any template agents, which enables us to control the material shape as well as the porous morphology. Several benefits are expected to arise from the ease, reproducibility and versatility of the present process.

2. Experimental procedure

2.1 Synthesis

Gel samples were obtained via the sol–gel route using metal salts of $YCl_3 \cdot 6H_2O$ (Aldrich, 99.99%) and $AlCl_3 \cdot 6H_2O$ (Aldrich, 99%) as the inorganic components, and a mixture of distilled water (H_2O) and ethanol (EtOH, Kishida Reagents Chemicals, 99.5%) as the solvent. Propylene oxide (PO, Aldrich, $\geq$99%) was added to initiate gelation, and poly(ethylene oxide) (PEO, Aldrich) having viscosity average molecular weight (M_v) of 1,000,000 was utilized as the polymer to induce the phase separation. All reagents were used as received.

The gels were prepared with the cation ratio of Y/Al = 3 : 5 so that stoichiometric $Y_3Al_5O_{12}$ could be formed upon heating at elevated temperature. The detail of gel preparation is as follows. First, 1.19 g $YCl_3 \cdot 6H_2O$ and 1.58 g of $AlCl_3 \cdot 6H_2O$, together with a given amount of PEO in the range of 0.02 to 0.09 g, were dissolved in a mixture of 4.0 g of H_2O and 2.37 g of EtOH. Then, 1.51 g of PO was added to the transparent solution under ambient conditions (25°C). After stirring for 1 min, the resultant homogeneous solution was transferred into a glass tube. The tube was sealed and kept at 40°C for gelation. After gelation, the wet gel was aged for 24 h and evaporation-dried at 40°C. Some of the dried gels were heat-treated at temperatures between 700 and 1000°C for 10 h in

air.

2.2 Characterization

Morphology of dried and heat-treated gels was observed by a scanning electron microscope (SEM; JSM-6060, JEOL, Pt–Pd coating) equipped with an energy-dispersive X-ray (EDX) spectrometer. X-ray diffraction (XRD) analysis with Cu Kα radiation ($\lambda = 0.154$ nm) (RINT-Ultima III, Rigaku Corp.) was performed in order to identify the crystalline phases precipitated. The measurements were carried out for the powder specimens prepared by grinding macroporous monoliths.

3. Results and discussion

The starting solutions were initially homogeneous and transparent. As time elapsed, the phase separation and the gelation proceeded spontaneously in a closed and static condition at a constant temperature (40°C). The gels prepared from the solution containing PO formed quite quickly (gelation time is ca. 15 min), although gelation did not take place in the solution without PO. As reported by Gash and co-workers,[6),14)] gelation of metal salts solution is induced by using epoxides as gelation initiators. Epoxides act as an irreversible proton scavenger, and cause the solution pH to increase gradually throughout the solution.[6)] The slow and uniform pH rise drives the hydrolysis and condensation of hydrated metal cations to form the monolithic gel. On the other hand, the addition of PEO to the starting solution did not have such a significant effect on the gelation time but instead induced the formation of phase-separated structures. When the PEO content was small, white and translucent gels were obtained. As the PEO content was increased, the gels became opaque white. **Figure 1** shows the SEM images of dried gels prepared with 0.02, 0.04, and 0.09 g of PEO. The gel morphology depends significantly on the PEO content. As the PEO content is increased, the gel morphology in the micrometer range changes from nonporous [Fig. 1(a)], through bicontinuous structure [Fig. 1(b)], to particle aggregates [Fig. 1(c)]. The variation of gel morphology with PEO content is mainly determined by the change in phase-separation tendency as mentioned below.

The phase separation tendency is related to the miscibility of a polymeric system, which can be estimated by the Flory-Huggins formulation.[15)–17)] The Gibbs free energy change of mixing, ΔG, can be described as follows;

$$\Delta G \propto RT \left(\frac{\phi_1}{P_1} \ln \phi_1 + \frac{\phi_2}{P_2} \ln \phi_2 + \chi \phi_1 \phi_2 \right) \qquad (1)$$

where χ is the interaction parameter, ϕ_i and P_i are the volume fraction and the degree of polymerization of component i ($i = 1$ or 2), respectively, R is the gas constant, and T is the temperature. The former two terms in parenthesis represent the entropic contribution, and the last term the enthalpic contribution. As we previously reported for the metal-salt-derived Al_2O_3 sol–gel system in the presence of PEO, entropy loss contributes essentially to ΔG, which causes the phase separation.[5)] Namely, either P_1 or P_2 in Eq. (1) becomes large as a result of the homogeneous condensation reaction of Al_2O_3 oligomers due to the uniform increase in solution pH, which makes ΔG large. In the present Y–Al–O system, aluminum hydroxide species are first formed at the early stage of the reaction, because aluminum hydroxide is less soluble than yttrium hydroxide in the acidic condition.[18)] In the following increase of solution pH, yttrium hydroxide species are precipitated preferentially onto the interfaces of aluminum hydroxide embryo and solution because of the local proton deficiency as in the case of co-precipitation method. The fine incorporation of yttrium hydroxide into the polymeric aluminum hydroxide is a key reaction, although further evidences are required. As reaction proceeds, the yttrium-incorporated aluminum species phase-separate due to the entropy loss during polymerization reaction. Since the addition of PEO to the starting solution reduces the compatibility between polymeric yttrium-incorporated aluminum species and PEO dissolved in the fluid phase composed mainly of solvent mixtures, the phase-separation tendency becomes strong with increasing PEO content. When the PEO content is small, phase separation does not occur effectively until gelation, and hence, transparent gels with nanometer-sized pores, i.e, nonporous gels in the micrometer range, are obtained [see Fig. 1(a)]. On the contrary, when the PEO content is too large, phase-separation tendency enhances significantly, which results in the fragmentation of the phase occupying a smaller volume fraction. In the present case, the minor phase is the gel phase, so that the sea-island structure, in which the fragmented gel phase is dispersed in the sea of fluid phase, is fixed by the gelation to form the spherical particle aggregates [Fig. 1(c)]. Nearly concurrent phase separation and gelation produce the bicontinuous monolithic structure [Fig. 1(b)], in which each of the gel phase and the fluid phase is three-dimensionally interconnected on the length scale of micrometers. After evaporation drying, the fluid phase composed mainly of solvent mixture turns into continuous macropores, and the gel phase becomes skeletons. Using this technique, one can obtain monolithic dried gel in large dimensions ($10 \times 10 \times 10$ mm). (see the inset of Fig. 1(b), where a circular cylinder with 10-mm diameter and 10-mm height is displayed).

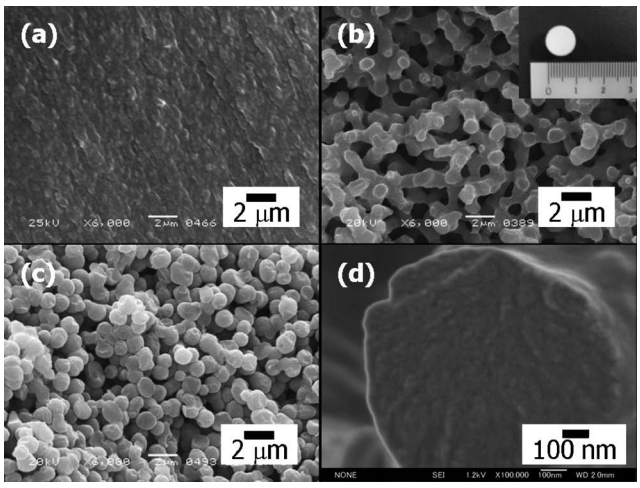

Fig. 1. SEM photographs of dried gels prepared with varied PEO content: (a) 0.02 g, (b) 0.04 g, and (c) 0.09 g of PEO. (d) FE-SEM photograph of dried gel prepared with 0.04 g of PEO.

Figure 1(d) corresponds to the FE-SEM image of the dried gel shown in Fig. 1(b). No precipitates or aggregates are observed for the gel skeleton, indicating the high homogeneity of resultant gels. Elemental analysis shown in **Fig. 2** also revealed no segregation of Y and Al, i.e., uniform distribution of Y^{3+} and Al^{3+}, in the gel skeleton.

Variation of XRD pattern with heat-treatment temperature is depicted in **Fig. 3**. The measurements were performed for the samples prepared with 0.04 g of PEO. For the dried gel, three broad diffraction peaks are observed at $2\theta = 10$, 24, and 40° [Fig. 2(a)], although the crystal structure can not be

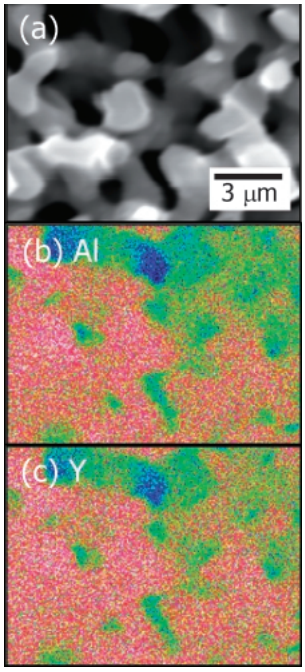

Fig. 2. Elemental mapping of the macroporous gel synthesized with 0.04 g of PEO: (a) SEM image, (b) aluminum map, and (c) yttrium map.

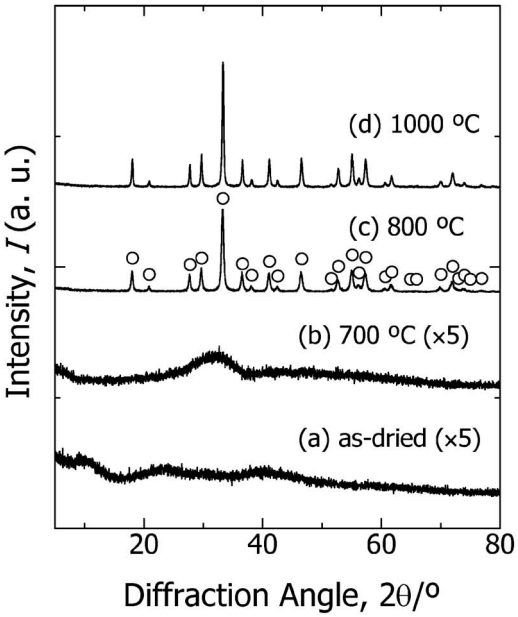

Fig. 3. Variation of XRD pattern with heat-treatment temperature. The measurements were carried out for the samples prepared with 0.04 g of PEO. Open circles represent the diffraction peaks ascribed to $Y_3Al_5O_{12}$ (YAG).

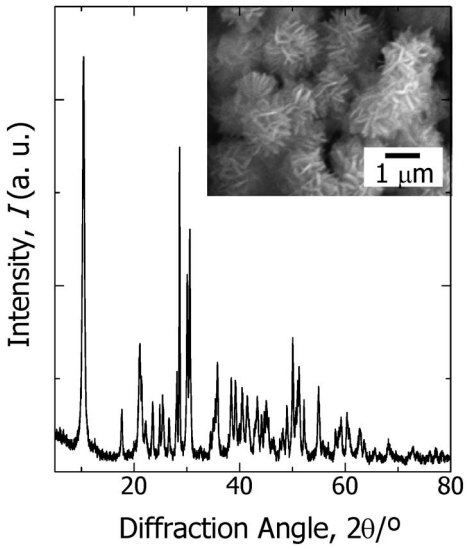

Fig. 4. XRD pattern of the precipitates prepared from 1.19 g of $YCl_3 \cdot 6H_2O$, 0.04 g of PEO, 4.0 g of H_2O, 2.37 g of EtOH, and 1.51 g of PO. The inset is the SEM image of the product, showing needle-like precipitates.

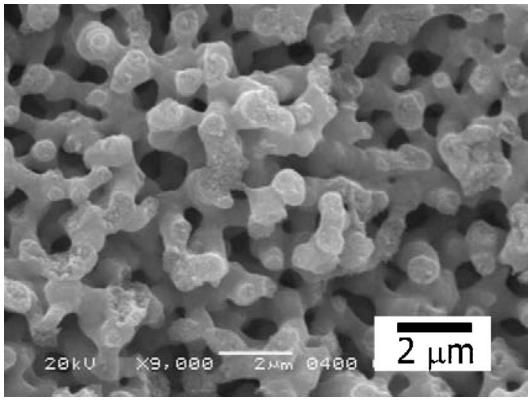

Fig. 5. SEM image of the gel prepared with 0.04 g of PEO and then heat-treated at 1000°C for 10 h.

exactly identified due to the poor crystallinity. As we reported previously, gels amorphous to X-ray were obtained from PO and $AlCl_3 \cdot 6H_2O$ in H_2O/EtOH solution.[5] On the other hand, as shown in **Fig. 4**, the addition of PO to $YCl_3 \cdot 6H_2O$ in H_2O/EtOH solution resulted in the formation of white needle-like precipitates ascribed to hydrated chloride-hydroxide precipitates with a general formula of $Y_2(OH)_{6-m}Cl_m \cdot nH_2O$, where m and n normally equal to one.[19] The observation that clear diffraction peaks ascribed to yttrium hydroxide are absent in the present Y–Al–O system indicates that yttrium hydroxide species are finely embedded into the polymeric aluminum hydroxide, suggesting that the segregation of yttrium hydroxide is significantly suppressed by coexistence with Al^{3+} species in the starting solution. The broad diffraction peaks disappear at 300°C, and halo pattern is observed up to 700°C [Fig. 3(b)]. Following heat treatment at temperature as low as 800°C [Fig. 3(c)], the diffraction peaks ascribed to YAG (JCPDS 33-0040) appear without the formation of any intermediate phases or the precipitation of impurity phases. Above 800°C, continued refinement of peak shapes and intensities is observed. The crystallite size estimated by Scherrer's equation using the (420) diffraction line is approximately 19.8 and 29.6 nm for samples heat-treated at 800 and 1000°C, respectively. Even after the heat treatment at 1000°C for 10 h, macroporous structure is maintained, as shown in **Fig. 5**. Namely, the bicontinuous macroporous network comprised of a single phase of YAG can be obtained by heating at temperatures above 800°C. According to thermogravimetry and

differential thermal analysis (not shown), the oxidation of residual organic components or the formation of Y–O–Al bonds through condensation and elimination of H_2O took place at temperatures below 900°C, while the removal of chlorine was observed at temperatures above 900°C. Thus, the chlorine impurity in macroporous YAG monoliths can be minimized by heat treatment above 900°C.

The synthesis of polycrystalline YAG using the conventional solid-state reaction usually requires heat treatment at 1600°C or so to obtain the single phase of YAG.[20] In contrast, co-precipitation approaches to synthesizing YAG nanoparticles using the metal salts have been shown to allow the transformation into YAG during heat treatment at temperatures below 1000°C in air.[18),21)–23)] For example, Wang et al.[18)] prepared Y–Al–O nanoparticulate gels from nitrate salts and ammonia solution, and observed the precipitation of YAG after subsequent heat treatment at 800°C. Li et al.[22)] reported that YAG nanoparticles can be obtained for the specimens prepared by using nitrate salts and ammonium hydrogen carbonate as starting materials, followed by heat treatment at 900°C. Obviously, the onset temperature of crystallization for the specimens derived from the present method is comparable to or lower than that for the specimens prepared via the co-precipitation method, which is again indicative of the uniform distribution of Y^{3+} and Al^{3+} ions at the stage of precursor gels.

4. Conclusions

YAG monoliths with well-defined macropores were prepared from the aqueous and ethanolic solution of yttrium and aluminum chlorides in the presence of PO and PEO using the sol–gel method accompanied by phase separation. Macroporous Y–Al–O nanocomposite precursor gels are formed by concurrent phase separation and sol-gel transition and can be transformed into nanocrystalline YAG by heat treatment at temperature as low as 800°C. The crystallization of YAG takes place without the formation of any intermediate phases or the precipitation of impurity phases, indicating high cation homogeneity of dried gels. Remarkably, the YAG monoliths are observed to maintain the macroporous morphology even after the heat treatment at 1000°C for 10 h. The integration of porous structures into robust monoliths would be beneficial, especially for the areas where processing or application dictates some structural form with moderate mechanical strength.

Acknowledgment This study was supported by the Grant-in-Aid for Scientific Research (No. 18360316) from the Ministry of Education, Culture, Sports, Science, and Technology (MEXT), Japan, and the Industrial Technology Research Grant Program (04A25023c) and the Grant for Practical Application of University R&D Results under the Matching Fund Method from the New Energy and Industrial Technology Development Organization (NEDO), Japan. K. F. thanks The Mazda Foundation for a research grant. Y. T. was supported by the research fellowship of global COE program, International Center for Integrated Research and Advanced Education in Material Science, Kyoto University, Japan.

References

1) K. Nakanishi, *J. Porous Mater.*, **4**, 67–112 (1997).
2) T. Amatani, K. Nakanishi, K. Hirao and T. Kodaira, *Chem. Mater.*, **17**, 2114–2119 (2005).
3) J. Konishi, K. Fujita, K. Nakanishi and K. Hirao, *Chem. Mater.*, **18**, 6069–6074 (2006).
4) J. Konishi, K. Fujita, S. Oiwa, K Nakanishi and K. Hirao, (*submitted*, 2007).
5) A. E. Gash, T. M. Tillotson, J. H. Satcher, Jr., J. F. Poco, L. W. Hrubesh and R. L. Simpson, *Chem. Mater.*, **13**, 999–1007 (2001).
6) Y. Tokudome, K. Fujita, K. Nakanishi, K. Miura and K. Hirao, *Chem. Mater.*, **19**, 3393–3398 (2007).
7) C. N. Chervin, B. J. Clapsaddle, H. W. Chiu, A. E. Gash. J. H. Satcher, Jr. and S. M. Kauzlarich, *Chem. Mater.*, **17**, 3345–3351 (2005).
8) B. T. Holland, C. F. Blanford and A. Stein, *Science*, **281**, 538–540 (1998).
9) A. Imhof and D. J. Pine, *Nature*, **389**, 948–951 (1997).
10) P. Yang, D. Zhao, D. I. Margolese, B. F. Chmelka and G. D. Stucky, *Nature*, **396**, 152–155 (1998).
11) E. L. Crepaldi, G. J. de A. A. Soler-Illia, A. Bouchara, D. Grosso, D. Durand and C. Sanchez, *Angew. Chem. Int. Ed.*, **42**, 347–351 (2003).
12) M. A. Carreon and V. V. Guliants, *Eur. J. Inorg. Chem.*, **1**, 27–43 (2005).
13) B. T. Holland, C. F. Blanford, T. Do and A. Stein, *Chem. Mater.*, **11**, 795–805 (1999).
14) T. F. Baumann, A. E. Gash, S. C. Chinn, A. M. Sawvel, R. S. Mawell and J. H. Satcher, Jr., *Chem. Mater.*, **17**, 395–401 (2005).
15) P. J. Flory, *J. Chem. Phys.*, **10**, 51–61 (1942).
16) M. Huggins, *J. Phys. Chem.*, **46**, 151–158 (1942).
17) M. Huggins., *Am. Chem. Soc.*, **64**, 1712–1719 (1942).
18) H. Wang, L. Gao and K. Niihara, *Mater. Sci. Eng. A* **288**, 1–4 (2000).
19) C. E. Holcombe, Jr., *J. Am. Ceram. Soc.*, **61**, 481–486 (1978).
20) D. R. Messier and G. E. Gazza, *Am. Ceram. Soc. Bull.*, **51**, 692–694 (1972).
21) V. B. Glushkova, O. N. Egorova, V. A. Krzhizhanovskaya and K. Y. Merezhinskii, *Inorg. Mater.*, **19**, 1015–1018 (1983).
22) J. G. Li, T. Ikegami, J. H. Lee, T. Mori and Y. Yajima, *J. Eur. Ceram. Soc.*, **20**, 2395–2405 (2000).
23) Q. Lu, W. Dong, H. Wang and X. Wang, *J. Am. Ceram. Soc*, **85**[2] 490–492 (2002).